

Knowledge Distillation with Refined Logits

Wujie Sun¹, Defang Chen^{1*}, Siwei Lyu²
Genlang Chen³, Chun Chen¹, Can Wang¹

¹Zhejiang University ²University at Buffalo ³NingboTech University
sunwujie@zju.edu.cn, defchern@zju.edu.cn

Abstract

Recent research on knowledge distillation has increasingly focused on logit distillation because of its simplicity, effectiveness, and versatility in model compression. In this paper, we introduce Refined Logit Distillation (RLD) to address the limitations of current logit distillation methods. Our approach is motivated by the observation that even high-performing teacher models can make incorrect predictions, creating a conflict between the standard distillation loss and the cross-entropy loss. This conflict can undermine the consistency of the student model’s learning objectives. Previous attempts to use labels to empirically correct teacher predictions may undermine the class correlation. In contrast, our RLD employs labeling information to dynamically refine teacher logits. In this way, our method can effectively eliminate misleading information from the teacher while preserving crucial class correlations, thus enhancing the value and efficiency of distilled knowledge. Experimental results on CIFAR-100 and ImageNet demonstrate its superiority over existing methods. The code is provided at <https://github.com/zju-SWJ/RLD>.

1 Introduction

Knowledge distillation (Gou et al. 2021) utilizes pre-trained high-performing teacher models to facilitate the training of a more compact student model. Compared to other model compression methods, such as pruning and quantization (Choudhary et al. 2020), knowledge distillation exhibits fewer constraints on the model architecture. This flexibility significantly broadens its applicability, contributing to its increasing prominence in recent research.

Hinton et al. (2015) were the first to introduce the concept of logit distillation. It is designed to align the logits of teacher and student models following the softmax operations, using Kullback-Leibler (KL) divergence as the alignment measure. Most subsequent research has maintained the original concept of logit distillation, instead focusing on exploring feature distillation (Romero et al. 2014; Komodakis and Zagoruyko 2017; Tian, Krishnan, and Isola 2020; Chen et al. 2021, 2022; Wang et al. 2022) in more depth, which specifically investigates the process of selecting and aligning intermediate-level features between teacher and student models. However, the potential architectural disparity between teacher and student models poses a significant chal-

lenge for feature alignment. This is mainly due to the fact that different architectures extract different features (Wang et al. 2022). Moreover, the extensive diversity in feature selection further amplifies the complexity of feature distillation and leads to an increase in training time in distillation (Chen et al. 2022). Recently, by decoupling the classical logit distillation loss, the study by Zhao et al. (2022) demonstrates that logit distillation can yield results that are on par with, or even superior to, those of feature distillation. Consequently, logit distillation has garnered considerable attention in the research community, thanks to its simplicity, effectiveness, and versatility.

However, despite the impressive achievements of recent logit distillation approaches (Li et al. 2023; Jin, Wang, and Lin 2023; Sun et al. 2024a), most overlook the impact of teacher prediction accuracy on the training process. Specifically, incorrect teacher predictions lead to a conflict between teacher loss and label loss, which may severely impede the potential for further enhancements of the student models. Existing correction-based distillation approaches (Wen, Lai, and Qian 2021; Cao et al. 2023; Lan et al. 2024) consistently modify the teacher logits (target) using label information. They either exchange the values between the predicted maximum class and the true class (Wen, Lai, and Qian 2021) (the *swap* operation) or amplify the proportion of the true class within the predicted probabilities (Cao et al. 2023; Lan et al. 2024) (the *augment* operation). We argue that such approaches may alter the correlation among classes, as exemplified in Figure 1. This disruption can obstruct the transmission of “dark knowledge” (Hinton, Vinyals, and Dean 2015) and hinder performance improvements.

We introduce *Refined Logit Distillation* (RLD) to address these challenges. RLD aims to alleviate the loss conflicts that arise in student training by empowering student models to assimilate valuable knowledge from their teachers. Specifically, RLD consists of two types of knowledge, *sample confidence* (SC) and *masked correlation* (MC). Sample confidence refers to the binary probabilities derived from logits. In the context of the teacher model, SC comes from the probability associated with the predicted class and the probabilities of the remaining classes. This metric encapsulates the teacher’s prediction confidence for the current sample and can be employed to guide the student model. Considering the possible inaccuracies in the teacher’s prediction,

*Corresponding author

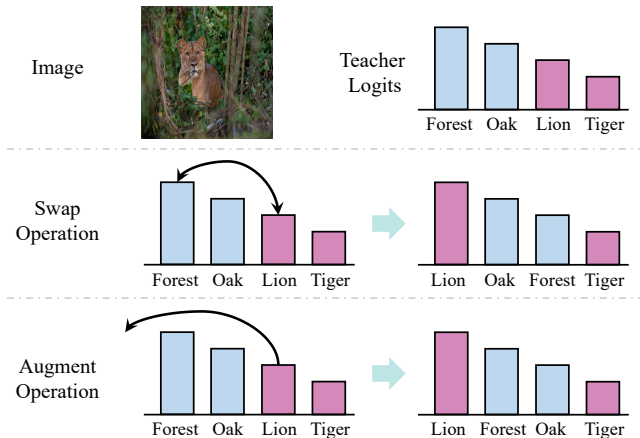


Figure 1: A toy example of existing correction-based distillation approaches. **Classes represented by the same color are closely related.** The image displayed is a “lion”, yet the teacher model incorrectly classifies it as the “forest”. Both the swap and augment operations disrupt the close correlation between “lion” and “tiger”. A more detailed example of class correlation is provided in the appendix.

we align the student’s true class prediction probability with that of the teacher’s. This alignment not only mitigates the mistakes by the teacher, but also guides the student model toward achieving a comparable level of confidence for the current sample. Moreover, it can effectively prevent overfitting. Masked correlation denotes our dynamic approach for selecting a subset of classes for teacher-student alignment. It is designed to mitigate the influence of potentially incorrect teacher predictions on student models while conveying essential class correlation. More specifically, MC involves masking all classes within the teacher logits that have equal or superior rankings compared to the true class. In essence, fewer classes are used for distillation when the teacher makes more mistakes (i.e., lower ranking for the true class), and more classes are used when it makes fewer mistakes. Using these two complementary types of refined knowledge, the student can achieve better performance.

Our contributions can be summarized as follows:

- We reveal that prevalent distillation approaches fail to account for the effects of incorrect teacher predictions, and existing correction-based strategies tend to ruin the valuable class correlation.
- We introduce a novel logit distillation approach termed Refined Logit Distillation (RLD) to prevent overfitting and mitigate the influence of incorrect teacher knowledge, while preserving the essential class correlation.
- We conduct comprehensive experiments on CIFAR-100 and ImageNet datasets to verify the superior performance of our proposed RLD method.

2 Related Work

The application of knowledge distillation historically concentrated on the image classification task, and progres-

sively extended to a wider range of tasks, including semantic segmentation (Liu et al. 2020; Shu et al. 2021; Yang et al. 2022; Sun et al. 2023b) and image generation (Salimans and Ho 2022; Sun et al. 2023a; Meng et al. 2023) within the realm of computer vision. Traditional knowledge distillation typically involves a single teacher and a single student model. As the field evolves, a variety of other paradigms have been proposed, such as online distillation (Chen et al. 2020; Wu and Gong 2021), multi-teacher distillation (Yuan et al. 2021; Zhang, Chen, and Wang 2022), and self-distillation (Furlanello et al. 2018; Kim et al. 2021; Sun et al. 2024b). Since traditional knowledge distillation remains the core foundation of research in this area, we will focus solely on such methods in the discussion below.

In image classification task, existing algorithms can be broadly classified into three categories: logit distillation, feature distillation (Komodakis and Zagoruyko 2017; Kim, Park, and Kwak 2018; Heo et al. 2019b; Tian, Krishnan, and Isola 2020; Chen et al. 2021; Wang et al. 2022; Chen et al. 2022), and relation distillation (Park et al. 2019; Liu et al. 2019; Peng et al. 2019). Logit distillation has become the main focus of current research because of its straightforwardness, effectiveness, and adaptability. The initial logit distillation (Hinton, Vinyals, and Dean 2015) leverages KL divergence to align the softened output logits of the teacher and student models, thereby significantly enhancing the performance of the student models. DKD (Zhao et al. 2022) revitalizes logit distillation by decoupling this classical loss, enabling it to perform comparably to feature distillation. MLKD (Jin, Wang, and Lin 2023) leverages multi-level logit knowledge to further enhance model performance. CTKD (Li et al. 2023) introduces the curriculum temperature, applying adversarial training and curriculum learning to dynamically determine the distillation temperature for each sample. LSKD (Sun et al. 2024a) processes the logits to adaptively allocate temperatures between teacher and student and across samples, thereby achieving state-of-the-art performance. However, the effect of incorrect teacher predictions on distillation is rarely considered.

Given that logits are intrinsically related to prediction accuracy, several methods leverage labels to adjust logits prior to the distillation process. LA (Wen, Lai, and Qian 2021) swaps the values of the true and predicted classes to correct the teacher model’s predictions. RC (Cao et al. 2023) amplifies the predicted value for the true class with the highest predicted probability in the student’s output distribution, thereby aiding the student model in making accurate and confident predictions. LR (Lan et al. 2024) combines one-hot labels with the teacher’s soft labels to produce a new, precise target for distillation. However, as previously demonstrated, these methods may disrupt class correlations, which can hinder performance improvement.

3 Preliminaries

We provide an overview of concepts related to knowledge distillation to facilitate readers’ understanding.

Consider an image classification task involving C classes. We have a pre-trained teacher model and a student model, denoted as θ^T and θ^S , respectively. For a single input image

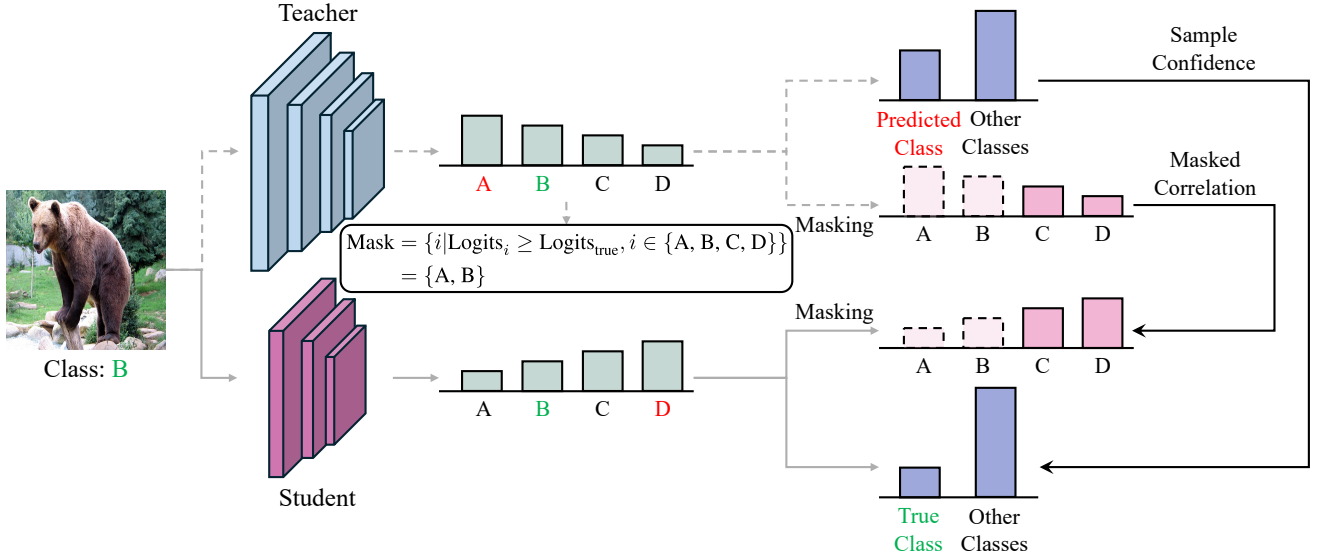


Figure 2: An overview of our proposed Refined Logit Distillation (RLD). In RLD, the teacher model imparts two types of knowledge, denoted as “sample confidence” and “masked correlation”, to the student model. Both kinds of knowledge are obtained from logits, thus the distillation process does not introduce intermediate layer features.

x , the output logits z from teacher and student models are denoted as $z^T = \theta^T(x)$ and $z^S = \theta^S(x)$, respectively. By utilizing the softmax function $\sigma(\cdot)$, predicted distributions p^T and p^S are calculated as follows:

$$p_i = \frac{\exp(z_i)}{\sum_{c=1}^C \exp(z_c)}, \quad (1)$$

where p_i represents the predicted value of the i -th class.

To train the student model, the first loss is computed as the cross entropy between the student prediction and the one-hot ground-truth label y :

$$L_{CE} = - \sum_{c=1}^C y_c \log p_c^S. \quad (2)$$

The second loss aligns the softened predictions $\hat{p} = \sigma(z/\tau)$ of the teacher and student models using the KL divergence:

$$L_{KD} = \tau^2 \text{KL}(\hat{p}^T, \hat{p}^S) = \tau^2 \sum_{c=1}^C \hat{p}_c^T \log \frac{\hat{p}_c^T}{\hat{p}_c^S}, \quad (3)$$

where τ denotes the temperature for the softmax operation.

By combining Eqs. 2 and 3, we get the classical logit distillation loss for stochastic gradient descent. Such an approach has been experimentally shown to perform better than training solely with labels.

4 Methodology

In this section, we delve into a detailed introduction of our proposed RLD. An overview of RLD is shown in Figure 2.

4.1 Sample Confidence Distillation

Sample confidence (SC) represents the binary distribution b derived from the logits. It encapsulates the model confidence for each sample, thereby aiding the student model in generating high-confidence predictions for the true class, without unduly restricting the distribution for other classes.

In the context of teacher knowledge, one component of the SC is the maximum predicted probability value \hat{p}_{\max}^T , while the other is the sum of predicted probabilities for the remaining classes. However, the student SC consists of the predicted probability for the true class \hat{p}_{true}^S , and the other includes the predicted probabilities for the remaining classes. They can be summarized in the following formulas:

$$b^T = \{\hat{p}_{\max}^T, 1 - \hat{p}_{\max}^T\}, \quad (4)$$

$$b^S = \{\hat{p}_{\text{true}}^S, 1 - \hat{p}_{\text{true}}^S\}. \quad (5)$$

To transfer this knowledge, we align b^T and b^S using the KL divergence:

$$L_{SCD} = \tau^2 \text{KL}(b^T, b^S). \quad (6)$$

Although entropy could potentially be employed to measure sample confidence, it would not be appropriate for our purpose. The aim of SC is to enable the student model to maintain a similar level of confidence for the true class without hindering the predicted probabilities of the other classes. However, a straightforward transfer of entropy does not impose this constraint on the true class of the student model, as shown in Figure 3(a) and (b).

4.2 Masked Correlation Distillation

Masked correlation (MC) denotes the probability distribution acquired after dynamically masking certain classes. As shown in Figure 3(c), this masking operation relieves

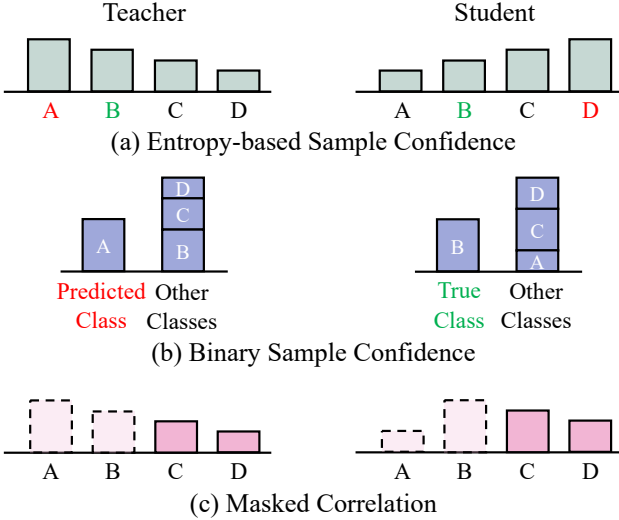


Figure 3: Toy examples elucidating the variances across methods when the teacher and student models are **well-aligned**. (a) Since entropy does not preserve the probability rank of different classes, it may cause incorrect student prediction. (b) Our proposed binary sample confidence guarantees a high probability for the true class and eliminates the necessity for the student model to match the intact class probability distribution to that of the teacher model. (c) Masked correlation imposes fewer constraints on the student prediction than traditional knowledge distillation. For the classes that are masked, their probabilities can diverge entirely from those of the teacher model.

| L_{SCD} | Mask | | Accuracy |
|-----------|-------|----------|----------|
| | M_g | M_{ge} | |
| | ✓ | | 75.50 |
| | | ✓ | 75.64 |
| ✓ | ✓ | | 75.53 |
| ✓ | | ✓ | 76.64 |

Table 1: Top-1 accuracy (%) on the CIFAR-100 validation set when training with different masking strategies. The teacher is ResNet32×4, and the student is ResNet8×4.

the student model from aligning incorrect class rankings, thereby allowing the student model to generate very different output from the teacher without incurring a large loss. Moreover, preserving partial class probabilities empowers the student model to learn valuable class correlation, consequently enhancing the model’s performance.

Specifically, the mask M is dynamically derived from teacher logits and labels. We designate all classes whose logit values are greater than or equal to (denoted as “ge”) the logit value of the true class as the targets for the masking operation, which can be represented as follows:

$$M_{ge} = \{i | z_i^T \geq z_{\text{true}}^T, 1 \leq i \leq C\}. \quad (7)$$

Although masking off all classes that have values greater

than (denoted as “g”) the true class would similarly remove the misinformation and preserve the class correlation, this masking strategy (denoted as M_g) inadvertently incorporate true class-related knowledge into both masked correlation and sample confidence. As demonstrated in the Table 1, this could potentially introduce conflicts among losses and impact the model performance. Hence, we opt for M_{ge} as the masking strategy.

After obtaining the mask, we compute the probability distributions for alignment using the following formula:

$$\tilde{p}_i = \frac{\exp(z_i/\tau)}{\sum_{c=1, c \notin M_{ge}}^C \exp(z_c/\tau)}, \quad (8)$$

where $1 \leq i \leq C$ and $i \notin M_{ge}$ are satisfied.

We summarize the distillation loss for the masked correlation knowledge as follows:

$$L_{MCD} = \tau^2 \text{KL}(\tilde{p}^T, \tilde{p}^S). \quad (9)$$

When the teacher model makes a more accurate prediction (ranking the true class higher), only a few classes are subjected to the masking operation. It allows the majority of class correlation to be preserved and transferred to the student model. Conversely, if the teacher’s prediction is less accurate, the majority of classes are masked. As a result, the student model learns less knowledge, thereby reducing the potential for misinformation to mislead the training process. It also gives the student model more freedom to make predictions for masked classes that differ significantly from those of the teacher model.

4.3 Refined Logit Distillation

By combining Eqs. 2, 6, and 9, we obtain the final loss for RLD, which is

$$L_{RLD} = L_{CE} + \alpha L_{SCD} + \beta L_{MCD}, \quad (10)$$

where α and β are hyper-parameters to adjust the importance of sample confidence and masked correlation, respectively. A detailed algorithm is shown in Algorithm 1, where temperature τ is omitted for concise.

Next, we elucidate the role of each loss function, which collaboratively enhances the model performance.

- L_{CE} encourages the student model to generate the highest probability for the true class, but it may cause over-fitting when deployed independently.
- L_{SCD} expects the student model to attain a reasonable level of confidence for the true class, thus averting over-fitting. However, when used in isolation, it could yield the probability assigned to one of the remaining classes exceeds that of the true class. When L_{CE} is amalgamated with L_{SCD} , the true class manages to retain the highest and most suitable probability. However, this combination falls short in transferring knowledge about the remaining classes.
- L_{MCD} lacks information about the true class (owing to the consistent masking of the true class), but it has the ability to eliminate misinformation and transfer valuable class correlation to the student model. By integrating L_{CE} and L_{SCD} with L_{MCD} , we can ensure the delivery of substantial valuable knowledge.

Algorithm 1: Refined Logit Distillation

Input: Training dataset $D = \{(x_n, y_n)\}_{n=1}^N$; Pre-trained teacher model θ^T ; Loss hyper-parameters α and β

Output: Student model θ^S

```
1: Randomly initialize  $\theta^S$ .
2: while not converged do
3:   for  $(x, y)$  in  $D$  do
4:     Propagate  $x$  forward through  $\theta$  to get logits  $z$ .
5:     Calculate  $L_{CE}$  using  $z^S$  and  $y$  (Eqs. 1 and 2).
6:     Obtain sample confidence  $b$  using  $z$  (Eqs. 4 and 5).
7:     Calculate  $L_{SCD}$  using  $b^T$  and  $b^S$  (Eq. 6).
8:     Obtain mask  $M_{ge}$  using  $z^T$  and  $y$  (Eq. 7).
9:     Obtain correlation  $\tilde{p}$  using  $z$  and  $M_{ge}$  (Eq. 8).
10:    Calculate  $L_{MCD}$  using  $\tilde{p}^T$  and  $\tilde{p}^S$  (Eq. 9).
11:    Calculate  $L_{RLD}$  with  $\alpha$  and  $\beta$  (Eq. 10).
12:    Backward  $L_{RLD}$  and update  $\theta^S$ .
13:  end for
14: end while
15: return  $\theta^S$ 
```

Relevance to DKD. Intriguingly, although our approach and DKD (Zhao et al. 2022) consider logit distillation from distinct perspectives, they become equivalent when the teacher model consistently makes accurate predictions. Besides, DKD does not explicitly elucidate why it is effective to underscore the non-target class knowledge, while our approach implies that by masking the true class during distribution alignment, the student model is provided with greater autonomy to adjust the ranking of the true class, thereby facilitating more accurate predictions.

5 Experiments

5.1 Settings

Datasets. We conduct the experiments on two standard image classification datasets: CIFAR-100 (Krizhevsky, Hinton et al. 2009) and ImageNet (Russakovsky et al. 2015). CIFAR-100 comprises 100 distinct classes, with a total of 50,000 images in the training set and 10,000 images in the validation set. Each image in this dataset is of the size 32×32 pixels. ImageNet presents a larger and more complex dataset, encompassing 1,000 classes. It includes 1.28 million images in the training set and 50,000 images in the validation set, with each image resolution being 224×224 pixels after pre-processing.

Models. Models used by teachers and students include ResNet (He et al. 2016), WideResNet (WRN) (Zagoruyko and Komodakis 2016), VGG (Simonyan and Zisserman 2015), ShuffleNet (SHN) (Ma et al. 2018; Zhang et al. 2018), and MobileNet (MN) (Howard et al. 2017; Sandler et al. 2018). The experimental results contain both the distillation of heterogeneous and homogeneous teacher-student models.

Compared Methods. The compared methods involved in the experiments include feature distillation and logit distillation methods. Feature distillation methods include FitNet (Romero et al. 2014), AT (Komodakis and Zagoruyko

2017), RKD (Park et al. 2019), CRD (Tian, Krishnan, and Isola 2020), OFD (Heo et al. 2019a), ReviewKD (Chen et al. 2021), SimKD (Chen et al. 2022), and CAT-KD (Guo et al. 2023). Logit distillation methods include KD (Hinton, Vinyals, and Dean 2015), CTKD (Li et al. 2023), DKD (Zhao et al. 2022), LA (Wen, Lai, and Qian 2021), RC (Cao et al. 2023), and LR (Lan et al. 2024). Notably, the latter three methods are based on correction techniques and are re-implemented by us in a unified training framework.

We follow the conventional experimental settings of previous works (Tian, Krishnan, and Isola 2020; Zhao et al. 2022; Sun et al. 2024a). For more details on implementation, please refer to the appendix.

5.2 Main Results

CIFAR-100. The top-1 validation accuracy (%) comparison results of RLD and other distillation approaches are reported in Table 2 (heterogeneous distillation pairs) and Table 3 (homogeneous distillation pairs). We can see that RLD is either the optimal or suboptimal logit distillation algorithm in all cases, and is optimal in most cases. This underscores the superiority of RLD and accentuates the significance of making corrections to teacher predictions. Concurrently, while feature distillation sometimes outperforms logit distillation, the optimal algorithm for feature distillation demonstrates greater instability, failing to perform well consistently with a certain algorithm. Moreover, feature distillation incurs a longer training duration and necessitates a more intricate algorithm design, potentially impeding its practical applicability.

ImageNet. The top-1 and top-5 validation accuracy (%) comparison results of RLD and other distillation approaches are reported in Table 4. On this more challenging dataset, RLD successfully outperforms all existing feature and logit distillation algorithms, consistently achieving optimal performance and demonstrating the superiority of our approach.

5.3 Visualizations

In this section, we use visualization to more intuitively represent the differences between the different methods. The teacher model is ResNet 32×4 , and the student model is ResNet 8×4 .

Feature Visualization. We employ the t-SNE (Van der Maaten and Hinton 2008) to visualize the output features of student models derived from KD and RLD. As depicted in Figure 4, the features obtained through RLD exhibit superior discriminative properties.

Logit Difference Visualization. We quantify the absolute difference in logits for each class between teacher and student models obtained via DKD and RLD, visualizing these results using the heat map in Figure 5. Despite RLD outperforming DKD, it is observed that the logit discrepancy yielded by RLD is larger than that of DKD. This observation aligns with our anticipation, given that RLD rectifies certain inaccuracies in teacher knowledge and provides students with greater autonomy in formulating their own predictions. This finding underscores that an unconsidered

| Type | Teacher | ResNet32×4 | ResNet32×4 | ResNet32×4 | WRN-40-2 | WRN-40-2 | VGG13 | ResNet50 |
|---------|------------|--------------|--------------|--------------|--------------|--------------|--------------|--------------|
| | Student | SHN-V2 | WRN-16-2 | WRN-40-2 | ResNet8×4 | MN-V2 | MN-V2 | MN-V2 |
| | | 79.42 | 79.42 | 79.42 | 75.61 | 75.61 | 74.64 | 79.34 |
| | | 71.82 | 73.26 | 75.61 | 72.50 | 64.60 | 64.60 | 64.60 |
| Feature | FitNet | 73.54 | 74.70 | 77.69 | 74.61 | 68.64 | 64.16 | 63.16 |
| | AT | 72.73 | 73.91 | 77.43 | 74.11 | 60.78 | 59.40 | 58.58 |
| | RKD | 73.21 | 74.86 | 77.82 | 75.26 | 69.27 | 64.52 | 64.43 |
| | CRD | 75.65 | 75.65 | 78.15 | 75.24 | 70.28 | 69.73 | 69.11 |
| | OFD | 76.82 | 76.17 | 79.25 | 74.36 | 69.92 | 69.48 | 69.04 |
| | ReviewKD | 77.78 | 76.11 | 78.96 | 74.34 | 71.28 | 70.37 | 69.89 |
| | SimKD | 78.39 | 77.17 | 79.29 | 75.29 | 70.10 | 69.44 | 69.97 |
| | CAT-KD | 78.41 | 76.97 | 78.59 | 75.38 | 70.24 | 69.13 | 71.36 |
| Logit | KD | 74.45 | 74.90 | 77.70 | 73.97 | 68.36 | 67.37 | 67.35 |
| | CTKD | 75.37 | 74.57 | 77.66 | 74.61 | 68.34 | 68.50 | 68.67 |
| | DKD | <u>77.07</u> | 75.70 | 78.46 | <u>75.56</u> | <u>69.28</u> | 69.71 | 70.35 |
| | LA | 75.14 | 74.68 | 77.39 | 73.88 | 68.57 | 68.09 | 68.85 |
| | RC | 75.61 | 75.17 | 77.58 | 75.22 | 68.72 | 68.66 | 68.98 |
| | LR | 76.27 | <u>76.10</u> | <u>78.73</u> | 75.26 | 69.02 | <u>69.78</u> | <u>70.38</u> |
| | RLD (ours) | 77.56 | 76.14 | 78.91 | 76.12 | 69.75 | 69.97 | 70.76 |

Table 2: Top-1 accuracy (%) on the CIFAR-100 validation set when the teacher and student models are heterogeneous. The best and second best results of logit distillation are highlighted in **bold** and underlined text, respectively. For the case where the best result of feature distillation is better than the best result of logit distillation, we highlight it with *italic* text. The reported results are the mean of three trials.

| Type | Teacher | ResNet32×4 | VGG13 | WRN-40-2 | WRN-40-2 | ResNet56 | ResNet110 | ResNet110 |
|---------|------------|--------------|--------------|--------------|--------------|--------------|--------------|--------------|
| | Student | ResNet8×4 | VGG8 | WRN-40-1 | WRN-16-2 | ResNet20 | ResNet32 | ResNet20 |
| | | 79.42 | 74.64 | 75.61 | 75.61 | 72.34 | 74.31 | 74.31 |
| | | 72.50 | 70.36 | 71.98 | 73.26 | 69.06 | 71.14 | 69.06 |
| Feature | FitNet | 73.50 | 71.02 | 72.24 | 73.58 | 69.21 | 71.06 | 68.99 |
| | AT | 73.44 | 71.43 | 72.77 | 74.08 | 70.55 | 72.31 | 70.65 |
| | RKD | 71.90 | 71.48 | 72.22 | 73.35 | 69.61 | 71.82 | 69.25 |
| | CRD | 75.51 | 73.94 | 74.14 | 75.48 | 71.16 | 73.48 | 71.46 |
| | OFD | 74.95 | 73.95 | 74.33 | 75.24 | 70.98 | 73.23 | 71.29 |
| | ReviewKD | 75.63 | 74.84 | 75.09 | 76.12 | 71.89 | 73.89 | 71.34 |
| | SimKD | 78.08 | 74.89 | 74.53 | 75.53 | 71.05 | 73.92 | 71.06 |
| | CAT-KD | 76.91 | 74.65 | 74.82 | 75.60 | 71.62 | 73.62 | 71.37 |
| Logit | KD | 73.33 | 72.98 | 73.54 | 74.92 | 70.66 | 73.08 | 70.67 |
| | CTKD | 73.39 | 73.52 | 73.93 | 75.45 | 71.19 | 73.52 | 70.99 |
| | DKD | <u>76.32</u> | <u>74.68</u> | <u>74.81</u> | 76.24 | <u>71.97</u> | 74.11 | 71.06 |
| | LA | 73.46 | 73.51 | 73.75 | 74.98 | 71.24 | 73.39 | 70.86 |
| | RC | 74.68 | 73.37 | 74.07 | 75.43 | 71.63 | 73.44 | <u>71.41</u> |
| | LR | 76.06 | 74.66 | 74.42 | 75.62 | 70.74 | 73.52 | 70.61 |
| | RLD (ours) | 76.64 | 74.93 | 74.88 | <u>76.02</u> | 72.00 | <u>74.02</u> | 71.67 |

Table 3: Top-1 accuracy (%) on the CIFAR-100 validation set when the teacher and student models are homogeneous. The same convention is used as in Table 2.

alignment with teacher knowledge may not be the optimal strategy, and we believe that correction-based approaches deserve more attention and research.

5.4 Extensions

Ablation Study. We perform ablation study on the components of RLD and the results are shown in Table 5. The

results demonstrate that each component of RLD effectively contributes to enhanced performance. Notably, when L_{SCD} or L_{MCD} are deployed separately (rows 2 and 3), the optimal results are achieved at different temperature settings. However, when integrating L_{SCD} and L_{MCD} (row 4), keeping the same temperature for both components outperforms setting different temperatures. This suggests that the interplay

| Teacher/Student | Res34/Res18 | | Res50/MN-V1 | |
|-----------------|--------------|--------------|--------------|--------------|
| Accuracy | Top-1 | Top-5 | Top-1 | Top-5 |
| Teacher | 73.31 | 91.42 | 76.16 | 92.86 |
| Student | 69.75 | 89.07 | 68.87 | 88.76 |
| AT | 70.69 | 90.01 | 69.56 | 89.33 |
| OFD | 70.81 | 89.98 | 71.25 | 90.34 |
| CRD | 71.17 | 90.13 | 71.37 | 90.41 |
| ReviewKD | 71.61 | <u>90.51</u> | <u>72.56</u> | 91.00 |
| SimKD | 71.59 | <u>90.48</u> | 72.25 | 90.86 |
| CAT-KD | 71.26 | 90.45 | 72.24 | <u>91.13</u> |
| KD | 71.03 | 90.05 | 70.50 | 89.80 |
| CTKD | 71.38 | 90.27 | 71.16 | 90.11 |
| DKD | <u>71.70</u> | 90.41 | 72.05 | 91.05 |
| LA | 71.17 | 90.16 | 70.98 | 90.13 |
| RC | 71.59 | 90.21 | 71.86 | 90.54 |
| LR | 70.29 | 89.98 | 71.76 | 90.93 |
| RLD (ours) | 71.91 | 90.59 | 72.75 | 91.18 |

Table 4: Top-1 and top-5 accuracy (%) on the ImageNet validation set. The best and second best results are highlighted in **bold** and underlined text, respectively. The reported results are the mean of three trials.

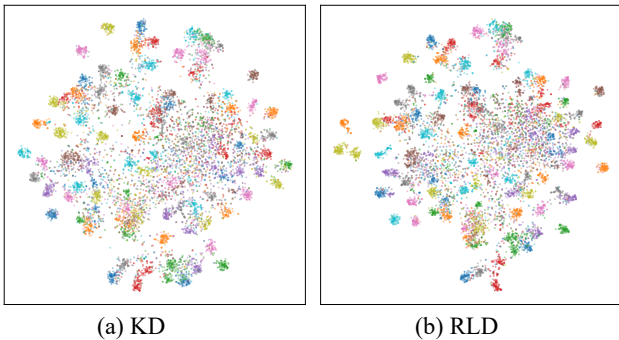


Figure 4: Visualized features learned by KD and RLD with t-SNE on the CIFAR-100 validation set.

of losses is also critical to achieving better performance.

Logit Standardization. We investigate the efficacy of each method when supplemented with logit standardization technique (Sun et al. 2024a). The results are shown in Table 6. The optimal results achieved by RLD underscore its superior performance and the vast potential of its integration with other methodologies.

6 Conclusion

Existing knowledge distillation methods did not consider the impact of incorrect teacher predictions on students, or arbitrarily corrected predictions and disrupted class correlation. In this paper, we introduce Refined Logit Distillation (RLD) to address these issues. RLD enables teacher models to impart two distinct forms of knowledge to the student models: sample confidence and masked correlation. It effectively

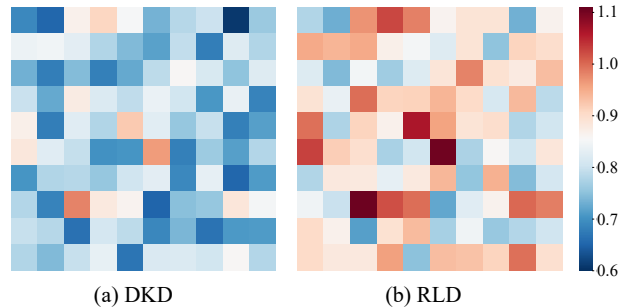


Figure 5: Visualized teacher-student logit difference learned by DKD and RLD on the CIFAR-100 validation set. To better display, 100 classes are reshaped into a 10×10 matrix.

| L_{CE} | L_{SCD} | L_{MCD} | Accuracy |
|----------|-----------|-----------|----------|
| ✓ | | | 72.50 |
| ✓ | ✓ | | 73.55 |
| ✓ | | ✓ | 75.64 |
| ✓ | ✓ | ✓ | 76.64 |

Table 5: Ablation study on the importance of each component in RLD. Top-1 accuracy (%) on the CIFAR-100 validation set is reported. The teacher is ResNet32 \times 4, and the student is ResNet8 \times 4.

| Teacher | WRN-40-2 | VGG13 | ResNet50 |
|------------|--------------|--------------|--------------|
| KD | 69.23 | 68.61 | 69.02 |
| CTKD | 69.53 | 68.98 | 69.36 |
| DKD | 70.01 | 69.98 | 70.45 |
| RLD (ours) | 70.35 | 70.63 | 71.06 |

Table 6: Top-1 accuracy (%) on the CIFAR-100 validation set when training with logit standardization technique. The student is MN-V2. The optimal results are highlighted in **bold** text. The reported results are the mean of three trials.

mitigates over-fitting and eliminates potential misinformation from the teacher models, while maintaining class correlation. Consequently, it enables student models to acquire more valuable knowledge. Experimental results demonstrate the superiority of our proposed method.

Future work. There are a few directions to improve our proposed RLD. For instance, dynamic temperature (Li et al. 2023) and meta-learning (Hospedales et al. 2021) techniques can be used to tune the hyper-parameters. Additional strategies such as data augmentation (Cubuk et al. 2019) and sample selection (Lan et al. 2024) can be employed to distill high-quality samples. Besides, combining RLD with state-of-the-art feature distillation methods may be a promising avenue of exploration to further improve the distillation performance. We consider extending correction-based knowledge distillation to the feature domain, utilizing techniques such as Class Activation Mapping (Wang et al. 2020).

References

- Cao, Q.; Zhang, K.; He, X.; and Shen, J. 2023. Be an Excellent Student: Review, Preview, and Correction. *IEEE Signal Processing Letters*, 30: 1722–1726.
- Chen, D.; Mei, J.-P.; Wang, C.; Feng, Y.; and Chen, C. 2020. Online knowledge distillation with diverse peers. In *Proceedings of the AAAI conference on artificial intelligence*, volume 34, 3430–3437.
- Chen, D.; Mei, J.-P.; Zhang, H.; Wang, C.; Feng, Y.; and Chen, C. 2022. Knowledge distillation with the reused teacher classifier. In *Proceedings of the IEEE/CVF conference on computer vision and pattern recognition*, 11933–11942.
- Chen, P.; Liu, S.; Zhao, H.; and Jia, J. 2021. Distilling knowledge via knowledge review. In *Proceedings of the IEEE/CVF Conference on Computer Vision and Pattern Recognition*, 5008–5017.
- Choudhary, T.; Mishra, V.; Goswami, A.; and Sarangapani, J. 2020. A comprehensive survey on model compression and acceleration. *Artificial Intelligence Review*, 53: 5113–5155.
- Cubuk, E. D.; Zoph, B.; Mane, D.; Vasudevan, V.; and Le, Q. V. 2019. Autoaugment: Learning augmentation strategies from data. In *Proceedings of the IEEE/CVF conference on computer vision and pattern recognition*, 113–123.
- Furlanello, T.; Lipton, Z.; Tschannen, M.; Itti, L.; and Anandkumar, A. 2018. Born again neural networks. In *International conference on machine learning*, 1607–1616. PMLR.
- Gou, J.; Yu, B.; Maybank, S. J.; and Tao, D. 2021. Knowledge distillation: A survey. *International Journal of Computer Vision*, 129(6): 1789–1819.
- Guo, Z.; Yan, H.; Li, H.; and Lin, X. 2023. Class attention transfer based knowledge distillation. In *Proceedings of the IEEE/CVF Conference on Computer Vision and Pattern Recognition*, 11868–11877.
- He, K.; Zhang, X.; Ren, S.; and Sun, J. 2016. Deep residual learning for image recognition. In *Proceedings of the IEEE conference on computer vision and pattern recognition*, 770–778.
- Heo, B.; Kim, J.; Yun, S.; Park, H.; Kwak, N.; and Choi, J. Y. 2019a. A comprehensive overhaul of feature distillation. In *Proceedings of the IEEE/CVF International Conference on Computer Vision*, 1921–1930.
- Heo, B.; Lee, M.; Yun, S.; and Choi, J. Y. 2019b. Knowledge transfer via distillation of activation boundaries formed by hidden neurons. In *Proceedings of the AAAI conference on artificial intelligence*, volume 33, 3779–3787.
- Hinton, G.; Vinyals, O.; and Dean, J. 2015. Distilling the knowledge in a neural network.
- Hospedales, T.; Antoniou, A.; Micaelli, P.; and Storkey, A. 2021. Meta-learning in neural networks: A survey. *IEEE transactions on pattern analysis and machine intelligence*, 44(9): 5149–5169.
- Howard, A. G.; Zhu, M.; Chen, B.; Kalenichenko, D.; Wang, W.; Weyand, T.; Andreetto, M.; and Adam, H. 2017. Mobilenets: Efficient convolutional neural networks for mobile vision applications.
- Jin, Y.; Wang, J.; and Lin, D. 2023. Multi-level logit distillation. In *Proceedings of the IEEE/CVF Conference on Computer Vision and Pattern Recognition*, 24276–24285.
- Kim, J.; Park, S.; and Kwak, N. 2018. Paraphrasing complex network: Network compression via factor transfer. *Advances in neural information processing systems*, 31.
- Kim, K.; Ji, B.; Yoon, D.; and Hwang, S. 2021. Self-knowledge distillation with progressive refinement of targets. In *Proceedings of the IEEE/CVF international conference on computer vision*, 6567–6576.
- Komodakis, N.; and Zagoruyko, S. 2017. Paying more attention to attention: improving the performance of convolutional neural networks via attention transfer. In *ICLR*.
- Krizhevsky, A.; Hinton, G.; et al. 2009. Learning multiple layers of features from tiny images.
- Lan, W.; Cheung, Y.-m.; Xu, Q.; Liu, B.; Hu, Z.; Li, M.; and Chen, Z. 2024. Improve Knowledge Distillation via Label Revision and Data Selection. *arXiv preprint arXiv:2404.03693*.
- Li, Z.; Li, X.; Yang, L.; Zhao, B.; Song, R.; Luo, L.; Li, J.; and Yang, J. 2023. Curriculum temperature for knowledge distillation. In *Proceedings of the AAAI Conference on Artificial Intelligence*, volume 37, 1504–1512.
- Liu, Y.; Cao, J.; Li, B.; Yuan, C.; Hu, W.; Li, Y.; and Duan, Y. 2019. Knowledge distillation via instance relationship graph. In *Proceedings of the IEEE/CVF Conference on Computer Vision and Pattern Recognition*, 7096–7104.
- Liu, Y.; Shu, C.; Wang, J.; and Shen, C. 2020. Structured knowledge distillation for dense prediction. *IEEE transactions on pattern analysis and machine intelligence*, 45(6): 7035–7049.
- Ma, N.; Zhang, X.; Zheng, H.-T.; and Sun, J. 2018. Shufflenet v2: Practical guidelines for efficient cnn architecture design. In *Proceedings of the European conference on computer vision (ECCV)*, 116–131.
- Meng, C.; Rombach, R.; Gao, R.; Kingma, D.; Ermon, S.; Ho, J.; and Salimans, T. 2023. On distillation of guided diffusion models. In *Proceedings of the IEEE/CVF Conference on Computer Vision and Pattern Recognition*, 14297–14306.
- Park, W.; Kim, D.; Lu, Y.; and Cho, M. 2019. Relational knowledge distillation. In *Proceedings of the IEEE/CVF conference on computer vision and pattern recognition*, 3967–3976.
- Paszke, A.; Gross, S.; Massa, F.; Lerer, A.; Bradbury, J.; Chanan, G.; Killeen, T.; Lin, Z.; Gimelshein, N.; Antiga, L.; et al. 2019. Pytorch: An imperative style, high-performance deep learning library. *Advances in neural information processing systems*, 32.
- Peng, B.; Jin, X.; Liu, J.; Li, D.; Wu, Y.; Liu, Y.; Zhou, S.; and Zhang, Z. 2019. Correlation congruence for knowledge distillation. In *Proceedings of the IEEE/CVF International Conference on Computer Vision*, 5007–5016.
- Romero, A.; Ballas, N.; Kahou, S. E.; Chassang, A.; Gatta, C.; and Bengio, Y. 2014. Fitnets: Hints for thin deep nets.
- Russakovsky, O.; Deng, J.; Su, H.; Krause, J.; Satheesh, S.; Ma, S.; Huang, Z.; Karpathy, A.; Khosla, A.; Bernstein, M.;

- et al. 2015. Imagenet large scale visual recognition challenge. *International journal of computer vision*, 115: 211–252.
- Salimans, T.; and Ho, J. 2022. Progressive distillation for fast sampling of diffusion models. In *International Conference on Learning Representations*.
- Sandler, M.; Howard, A.; Zhu, M.; Zhmoginov, A.; and Chen, L.-C. 2018. Mobilenetv2: Inverted residuals and linear bottlenecks. In *Proceedings of the IEEE conference on computer vision and pattern recognition*, 4510–4520.
- Shu, C.; Liu, Y.; Gao, J.; Yan, Z.; and Shen, C. 2021. Channel-wise knowledge distillation for dense prediction. In *Proceedings of the IEEE/CVF International Conference on Computer Vision*, 5311–5320.
- Simonyan, K.; and Zisserman, A. 2015. Very deep convolutional networks for large-scale image recognition. In *International Conference on Learning Representations*. Computational and Biological Learning Society.
- Sun, S.; Ren, W.; Li, J.; Wang, R.; and Cao, X. 2024a. Logit standardization in knowledge distillation. In *Proceedings of the IEEE/CVF Conference on Computer Vision and Pattern Recognition*, 15731–15740.
- Sun, W.; Chen, D.; Wang, C.; Ye, D.; Feng, Y.; and Chen, C. 2023a. Accelerating diffusion sampling with classifier-based feature distillation. In *2023 IEEE International Conference on Multimedia and Expo (ICME)*, 810–815. IEEE.
- Sun, W.; Chen, D.; Wang, C.; Ye, D.; Feng, Y.; and Chen, C. 2023b. Holistic Weighted Distillation for Semantic Segmentation. In *2023 IEEE International Conference on Multimedia and Expo (ICME)*, 396–401. IEEE.
- Sun, W.; Chen, D.; Wang, C.; Ye, D.; Feng, Y.; and Chen, C. 2024b. Multi-exit self-distillation with appropriate teachers. *Frontiers of Information Technology & Electronic Engineering*, 25(4): 585–599.
- Sutskever, I.; Martens, J.; Dahl, G.; and Hinton, G. 2013. On the importance of initialization and momentum in deep learning. In *International conference on machine learning*, 1139–1147. PMLR.
- Tian, Y.; Krishnan, D.; and Isola, P. 2020. Contrastive Representation Distillation. In *International Conference on Learning Representations*.
- Van der Maaten, L.; and Hinton, G. 2008. Visualizing data using t-SNE. *Journal of machine learning research*, 9(11).
- Wang, C.; Chen, D.; Mei, J.-P.; Zhang, Y.; Feng, Y.; and Chen, C. 2022. SemCKD: Semantic calibration for cross-layer knowledge distillation. *IEEE Transactions on Knowledge and Data Engineering*.
- Wang, H.; Wang, Z.; Du, M.; Yang, F.; Zhang, Z.; Ding, S.; Mardziel, P.; and Hu, X. 2020. Score-CAM: Score-weighted visual explanations for convolutional neural networks. In *Proceedings of the IEEE/CVF conference on computer vision and pattern recognition workshops*, 24–25.
- Wen, T.; Lai, S.; and Qian, X. 2021. Preparing lessons: Improve knowledge distillation with better supervision. *Neurocomputing*, 454: 25–33.
- Wu, G.; and Gong, S. 2021. Peer collaborative learning for online knowledge distillation. In *Proceedings of the AAAI Conference on artificial intelligence*, volume 35, 10302–10310.
- Yang, C.; Zhou, H.; An, Z.; Jiang, X.; Xu, Y.; and Zhang, Q. 2022. Cross-image relational knowledge distillation for semantic segmentation. In *Proceedings of the IEEE/CVF Conference on Computer Vision and Pattern Recognition*, 12319–12328.
- Yuan, F.; Shou, L.; Pei, J.; Lin, W.; Gong, M.; Fu, Y.; and Jiang, D. 2021. Reinforced multi-teacher selection for knowledge distillation. In *Proceedings of the AAAI Conference on Artificial Intelligence*, volume 35, 14284–14291.
- Zagoruyko, S.; and Komodakis, N. 2016. Wide Residual Networks. In *British Machine Vision Conference*. British Machine Vision Association.
- Zhang, H.; Chen, D.; and Wang, C. 2022. Confidence-aware multi-teacher knowledge distillation. In *ICASSP 2022-2022 IEEE International Conference on Acoustics, Speech and Signal Processing (ICASSP)*, 4498–4502. IEEE.
- Zhang, X.; Zhou, X.; Lin, M.; and Sun, J. 2018. Shufflenet: An extremely efficient convolutional neural network for mobile devices. In *Proceedings of the IEEE conference on computer vision and pattern recognition*, 6848–6856.
- Zhao, B.; Cui, Q.; Song, R.; Qiu, Y.; and Liang, J. 2022. Decoupled knowledge distillation. In *Proceedings of the IEEE/CVF Conference on computer vision and pattern recognition*, 11953–11962.

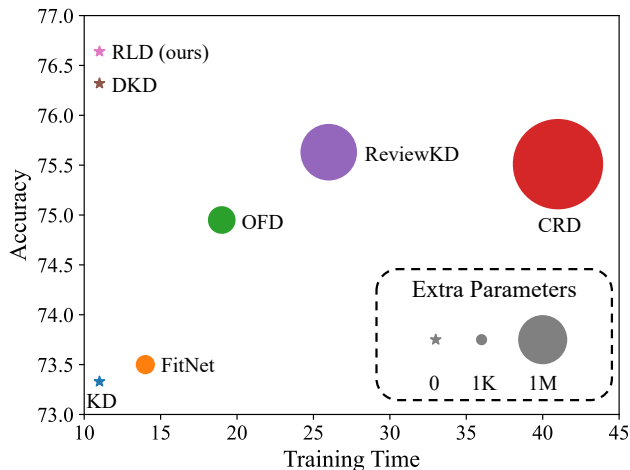


Figure 6: Batch training time (ms) vs. top-1 validation accuracy (%) on the CIFAR-100 dataset. The teacher is ResNet32×4, and the student is ResNet8×4. Larger circle denotes more extra parameters.

A Training Efficiency

Figure 6 presents the training time, accuracy, and extra parameters of various methods. Notably, feature distillation methods (FitNet, OFD, ReviewKD, and CRD) yield a substantial performance enhancement compared to traditional KD method, albeit at the cost of a significant increase in training time and extra parameters. In contrast, our RLD method, maintaining the same training time as KD without extra parameters introduced, delivers superior performance.

B Implementation Details

We follow the conventional experimental settings of previous works (Tian, Krishnan, and Isola 2020; Zhao et al. 2022; Sun et al. 2024a) and use Pytorch (Paszke et al. 2019) for our experiments.

B.1 CIFAR-100

When training on CIFAR-100, the batch size, epoch number, weight decay, and momentum are set to 64, 240, 5e-4, and 0.9, respectively. The initial learning rates are 0.01 for ShuffleNet and MobileNet, and 0.05 for other model architectures. The learning rate is divided by 10 at 150, 180 and 210 epochs. The optimizer is SGD (Sutskever et al. 2013). The training data is augmented using RandomCrop and RandomHorizontalFlip operators.

For the hyper-parameters involved in RLD, we follow DKD (Zhao et al. 2022) and LSKD (Sun et al. 2024a) to set different values for different distillation pairs. We always set α to 1, and determine the optimal β and τ using grid search from the range of $\{2, 4, 8, 16\}$ and $\{2, 3, 4, 5\}$, respectively.

Our experiments are carried out on the server equipped with NVIDIA GeForce RTX 2080 Ti GPUs. Each GPU has 11 GB of memory. Only one GPU is used per experiment. The server’s operating system is Ubuntu 18.04 LTS.

B.2 ImageNet

When training on ImageNet, the batch size, epoch number, weight decay, and momentum are set to 512, 100, 1e-4, and 0.9, respectively. The initial learning rate is 0.2 and divided by 10 for every 30 epochs. The optimizer is SGD (Sutskever et al. 2013). The training data is augmented using RandomResizedCrop and RandomHorizontalFlip operators.

For the hyper-parameters involved in RLD, we follow DKD (Zhao et al. 2022) and LSKD (Sun et al. 2024a) to set different values for different distillation pairs. We always set α to 1, and determine the optimal β and τ using grid search from the range of $\{0.5, 1, 2, 3\}$ and $\{1, 2\}$, respectively.

Our experiments are carried out on the server equipped with NVIDIA A100 Tensor Core GPUs. Each GPU has 80 GB of memory. Only one GPU is used per experiment. The server’s operating system is Ubuntu 18.04 LTS.

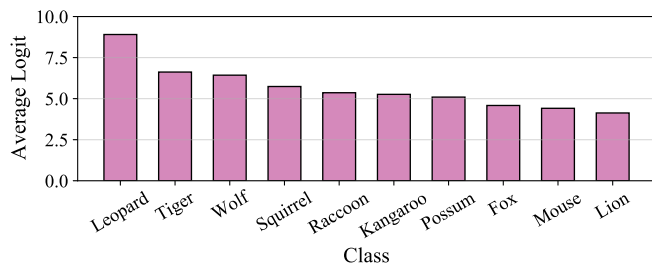
C Class Correlation

In this section, we present results from a pilot experiment, affirming the existence of scenarios similar to the one depicted in Figure 1 do indeed occur. We choose samples specifically from 3 classes in CIFAR-100: leopard, television, and dinosaur. Utilizing a well-trained model, we obtain the top 10 output logits. The corresponding results are displayed in Figure 7.

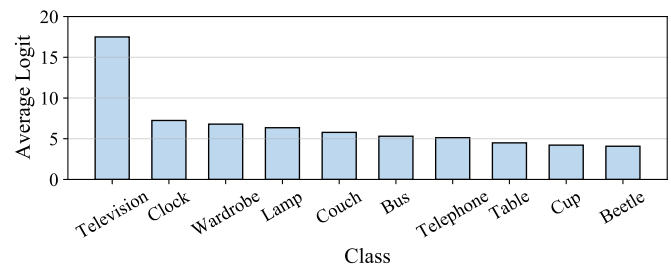
Figures 7(a), (b), and (c) illustrate that the model’s class correlation aligns with our understanding, regardless of whether the prediction is correct or not. For instance, leopard exhibits higher similarity to tiger, while television resemble clock more closely. When examining the overall samples, if the label is “leopard”, the model cannot enhance prediction confidence or accuracy by decreasing the logit values of its actual similar classes (such as “tiger”).

Figure 7(d) reveals that even in the output logits of a single sample, this inter-class relationship is well-maintained. For the sample labeled “dinosaur”, the top 2 predictions are “leopard” and “television”. Consequently, within its top 10 predicted classes, the proportion of classes similar to “leopard” or “television” is significantly high, while classes resembling “dinosaur” are rare. In such a scenario, merely correcting the true class would lead to an adjusted prediction that dinosaur are most similar to leopard (augment operation (Cao et al. 2023; Lan et al. 2024)) or television (swap operation (Wen, Lai, and Qian 2021)), which starkly contradicts the overall class-correlation observed in Figure 7(c).

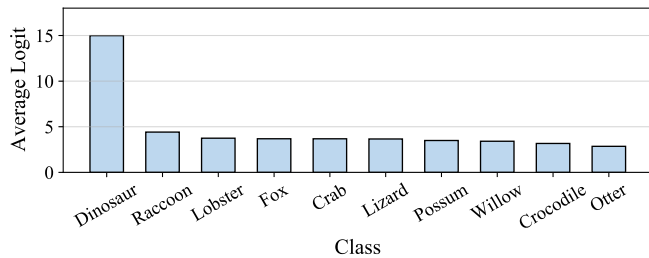
However, our proposed RLD can eliminate all classes with larger logit values than “dinosaur”, enabling the model to correct the prediction based on its existing knowledge without disrupting the class correlation.



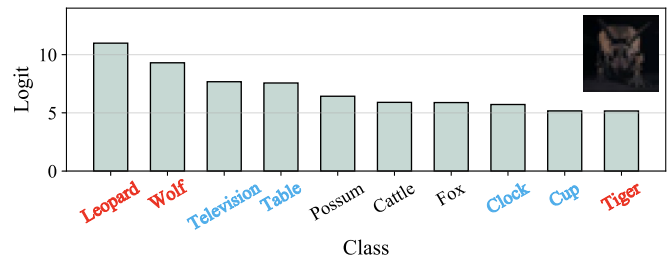
(a) Results based on **incorrect** samples for “leopard”



(b) Results based on **correct** samples for “television”



(c) Results based on **correct** samples for “dinosaur”



(d) Results based on **single incorrect** sample for “dinosaur”

Figure 7: Prediction results for different classes on the CIFAR-100 validation set. The model for calculation is ResNet110. Bold colored classes in (d) denote that they are among the top 10 classes most similar to either “leopard” (as inferred from (a)) or “television” (as inferred from (b)), yet they do not appear in the top 10 classes most similar to “dinosaur” (as inferred from (c)).